IgMin RESEARCH
A BioMed & Engineering Journal
Focusing on Biology, Medicine and Engineering disciplines
ENGINEERING
ISSN 2995-8067
Materials Science | Structural Engineering | Energy System

Article Information

Submitted: February 02, 2024
Approved: November 01, 2024
Published: November 04, 2024

How to cite this article: Yousuf M, Qadri SB. High Resolution X-ray Diffraction Studies of the Natural Minerals of Gas Hydrates and Occurrence of Mixed Phases. IgMin Res. November 04, 2024; 2(11): 889-896. IgMin ID: igmin265; DOI: 10.61927/igmin265; Available at: igmin.link/p265

Copyright: © 2024 Yousuf M, et al. This is an open access article distributed under the Creative Commons Attribution License, which permits unrestricted use, distribution, and reproduction in any medium, provided the original work is properly cited.

Keywords: Clathrate hydrates of natural gases; High-resolution X-ray diffraction; Structure I; Structure II; Structure H; Ice Ih

Check for updates

Review Article

High Resolution X-ray Diffraction Studies of the Natural Minerals of Gas Hydrates and Occurrence of Mixed Phases

M Yousuf[1] and SB Qadri[2]*

[1]The George Washington University, Washington, DC 20052, USA
[2]Emeritus, U. S. Naval Research Laboratory, Washington, DC 20375, USA

***Correspondence:** SB Qadri, Emeritus, U. S. Naval Research Laboratory, Washington, DC 20375, USA, Email: syed.b.qadri.ctr@nrl.navy.mil

Abstract

The types and concentrations of gas hydrates collected from four different geological sites were analyzed using high-resolution angular dispersive X-ray powder diffraction, with synchrotron radiation as the source. Measurements were taken across a temperature range of 80 to 300 K and a pressure range of 0.1 to 80 MPa. All four gas hydrate samples showed the presence of three mixed crystal structures: structures I, II, and H. Additionally, the ice Ih structure was inherently present in all the natural gas hydrate minerals. The variation in the types and concentrations of gas hydrates can be attributed to the diversity of natural gases at different geographic locations.

Introduction

Gas hydrates form when natural gases migrate from beneath the seafloor along natural faults and precipitate or crystallize upon contact with cold seawater at pressures of several tens of MPa [1-5]. Although gas hydrates can be synthesized in the laboratory, the experiments suggest the formation of a single phase due to the controlled growth parameters and the reactants in nature. For example, laboratory experiments can be controlled to produce a clathrate hydrate of natural gas in a purely single structure type [6-10]. However, achieving this in nature is rarely possible. This is because the crystalline states obtained on the seafloor depend on four major geophysical, organo-chemical, and microbiological field variables: (1) the type and concentration of natural gases present and their migration rates, (2) the temperature and pressure of seafloor water, (3) the concentration of living and non-living non-water bodies, and (4) the prevailing hydrodynamics and other physical variables of the seafloor water environment.

Gas hydrates, or clathrate hydrates of natural gases, are solid-like minerals formed at low temperatures and high pressures by van der Waals forces between gas and water molecules. The host water molecules form molecular cages that trap the guest gas molecules through mutual electrostatic interactions. These hydrates contain natural gases, such as hydrocarbons, which are encapsulated within the water molecule cages.

Although clathrate hydrates of natural gases contain colorless hydrocarbons, not all of them appear milky white like snow. For instance, hydrates from the Gulf of Mexico are often richly colored in shades of yellow, orange, or red, while samples from the Cascadia Margin are almost entirely milky white. The origin of the coloration is not fully understood, but it is believed that the presence of oil, bacteria, and minerals all play a role. In the ocean, gas hydrates, which are predominantly composed of methane, are common constituents of the shallow marine geosphere and occur both as deep sedimentary structures and as outcrops on the ocean floor.

Natural gas hydrates are found globally in marine sediments, permafrost regions, and continental ice sheets. Their formation depends on the presence of sufficiently high concentrations of natural gases such as methane and more complex hydrocarbons, along with elevated pressures and reduced temperatures. Methane is primarily produced through the fermentative decomposition of organic matter or the bacterial reduction of CO_2 in sediments. The thermo-

ISSN 2995-8067 DOI: 10.61927/igmin265

catalytic conversion of organic matter in the deeper subsurface can also be an equally important source of methane and more complex hydrocarbons. In this case, methane may migrate from deeper sources into the hydrate stability zone [11]. Large hydrate deposits are found along continental margins, where their formation is favored by rapid sedimentation and high sedimentary organic matter content. On land, stable methane hydrates in permafrost regions likely result from the natural migration of gases from deeper hydrocarbon reservoirs. Methane hydrates are also found in polar ice sheets, forming at depth due to air inclusions [12].

Hydrocarbons captured in natural gas hydrates predominantly consist of methane [13-15]. Based on their sizes and their ability to interact with water, the condensed matter state of hydrophobic (hydrocarbon) gas molecules with water can be classified into five types [16-20]:

1. **Smallest guest atoms and molecules:** These include hydrogen, helium, and neon (molecular diameter, d<3.5A°). They can form solid solutions based on ice Ih or, at high pressure, hydrates based on ice II and ice Ic.

2. **Slightly larger guest molecules:** This group includes Ar, Kr, O_2, and N_2 (molecular diameter, 3.5 A°<d<4.2 A°. At relatively low pressure, they form hydrates with structure II (sII), a face-centered cubic structure in the space group Fd3m. The unit cell contains eight hexakaidecahedral H ($5^{12}6^4$) and sixteen pentagonal-dodecahedral D (5^{12}) cavities, which are occupied by the guest molecules (Figure 1(a)).

3. **Medium-sized guest molecules:** Examples include H_2S, SO_2, CO_2, Xe, and C_2H_6, satisfying the criterion 4.3 A°<d<5.8 A°. These molecules stabilize hydrate structure I (sI), a simple cubic structure belonging to the space group Pm3n. The unit cell consists of two D and six tetrakaidecahedral T ($5^{12}6^2$) cavities (Figure 1(b)).

4. **Larger guest molecules:** These molecules, with diameters 5.8 A°<d<7.2 A, form sII hydrates where only the H cavities are occupied while the D cavities remain vacant.

5. **Very large guest molecules:** Examples include methylcyclohexane and adamantane. These molecules form structure H (sH), a simple hexagonal structure in the space group P6/mmm. The unit cell consists of three types of cavities: three regular dodecahedral D, two irregular dodecahedral D' ($4^35^66^3$), and one regular icosahedral E ($5^{12}6^8$) (Figure 1(c)). Structure H is stable only in the presence of a helper gas such as methane, which occupies the D and D' cavities.

The research presented in this paper focuses on the study of clathrate hydrates of natural gases collected from various

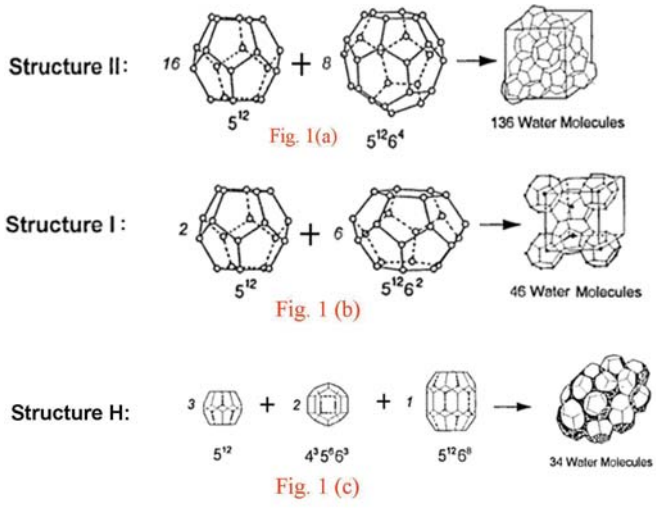

Figure 1: Unit cells of hydrate structures II (a), I (b), and H (c). The building blocks are in the form of cages formed by water molecules. Structures I and II have two types of cages; structure H has three types of cages.

geographic locations in the Pacific, Atlantic, and Arctic Oceans. This study was undertaken for three main reasons: (1) structural information is crucial for designing and developing technology to extract this extensive frozen energy resource from the seafloor in an economically viable manner, (2) comprehensive structural data on these natural minerals are currently lacking to our knowledge, and (3) laboratory experiments have not fully replicated the complex natural processes responsible for hydrate formation. Our research specifically emphasizes structural investigations of these natural clathrate hydrate minerals.

Experimental and data acquisition strategies

Using Department of Navy submarine vessels, clathrate hydrates of natural gases were collected from five distinct geographical locations: (1) the Texas-Louisiana Shelf in the Gulf of Mexico, (2) the Nankai Trough off the Eastern Coast of Japan, (3) the Blake Ridge in the Northwestern Atlantic Ocean, (4) the Cascadia Margin in the Northeastern Pacific Ocean, and (5) the Hakkon-Mosby Mud Volcano in the Norwegian-Greenland Sea. During submarine dives, naturally occurring gas hydrates were retrieved from approximately 600 meters depth. These hydrates were transferred into plastic bags and stored in an LN2 dewar to maintain their natural state.

A flat, sturdy metallic platform, kept near LN2 temperature, supported a pestle-mortar combination used to finely powderize the hydrates from the LN2 dewar. The resulting powder was filtered through a fine wire-mesh (<200 μm) to isolate the desired samples. An aluminum piston-cylinder assembly, with dimensions of 12 mm inner diameter and 25 mm length, capable of withstanding pneumatic pressures up to ~100 MPa, was loaded with the sample and promptly transferred to a closed cycle refrigerator (CCR) attached to the BESSRC CAT ID 11-D beamline at the Advanced Photon Source

ISSN 2995-8067 DOI: 10.61927/igmin265

(APS), Argonne National Laboratory. The 11-ID-D beamline features a modified BESSRC double crystal monochromator covering an energy range of 4.0 to 40 keV, utilizing a cryo-cooled Si(220) crystal with a 20 mm fixed offset. The incident beam was focused by a Pt-coated toroidal mirror with a 2.8 mrad incident angle [21]. The CCR maintained sample temperatures between 80 and 300 K, with pressure and temperature stabilities observed at 0.01 MPa and 1 K, respectively.

Temperature variations across the sample were monitored using two thermocouples placed at the ends of the pressure cell, ensuring a temperature difference of less than 3 K before data acquisition. The incident beam energy was optimized at 25 keV (λ = 0.49592 Å) to achieve the best resolution, largest interplanar spacing, and highest signal-to-noise ratio.

Initial experiments involved blank cell measurements to establish peak positions using aluminum as the reference. Subsequently, X-ray powder standards of Al, Al_2O_3, and ice were employed for diffractometer calibration to ensure precision and accuracy. Lattice parameter resolution was approximately 10^{-4} Å with accuracy better than 10^{-3} Å.

High-resolution X-ray diffraction data were acquired using a scintillation counter detector positioned approximately 300 mm from the sample. Data collection utilized a 2θ-step of 0.01° with each point measured for 3 seconds within the range 1.5° ≤ 2θ ≤ 30°. Following sample pressurization with high-purity nitrogen gas (4 to 80 MPa), accurate 2θ values and peak intensities were determined using XFIT, a peak profile-fitting program. The majority of diffraction peaks were fitted with pseudo-Voigt distributions, while some required Gaussian and Lorentzian fits. XRDA, a least squares fitting program, was used to analyze the diffraction data sets, identifying peaks corresponding to ice Ih, and clathrate hydrate structures sI, sII, and sH.

Structure refinements incorporated lattice parameters from XRDA output, symmetry positions based on NMR findings, and atomic positions (oxygen, half-hydrogen, carbon, and hydrogen) sourced from single crystal X-ray and neutron diffraction literature, employing covalent radii throughout the refinement process. Iterative refinement steps were undertaken to optimize agreement between experimental and observed intensity data.

Results and discussions

First, we describe the hydrocarbon composition and stable carbon isotope data on the hydrate minerals. Since, the formation, stability and dissociation energy of hydrates are functions of biological, chemical, and physical conditions, we performed these two measurements. The hydrocarbon composition data are presented in Table 1 and it is noted that the hydrate minerals consist of a broad range of gases. The stable carbon isotope analyses for hydrocarbons (CH_4 to C_4H_{10}) and CO_2 indicate that in the samples from the Gulf of Mexico and Haakon Mosby Mud Volcano, the value of $d^{13}C$ in CH_4 is in the range of -60 to -50, implying that these minerals have biogenic origin. In the following, representative structural results on natural minerals of gas hydrates obtained from three geographical locations are presented.

Hydrates of cascadia margin, Northeastern Pacific Ocean

The natural minerals collected from the Northern Pacific Ocean Play were found to exhibit a notable concentration of methane, attributed to a biogenic origin. A representative diffractogram at a temperature of 150 K is depicted in Figure 2.

Table 2 lists the experimental d-spacings. The lattice parameters for ice Ih (Space Group P63/mmc) are: a = 4.5115 ± 0.0068 Å and c = 7.3566 ± 0.0001 Å. For the clathrate hydrate in sI, the lattice parameter is a = 11.9132 ± 0.0235 Å. The predominant structure of the clathrate hydrates of natural gas samples obtained from the Cascadia Margin is cubic, with the space group Pm3n. It is noteworthy that natural

Table 1: Hydrocarbon content in hydrate samples from the Taxas-Louisiana Shelf in the Gulf of Mexico and the Haakon-Mosby Mud Volcano in the Norwegian Greenland Sea. Bush Hill and Green Canyon are located in the Gulf of Mexico. Yellow hydrates have Petroleum present between the clathrate structures.

Sample identification	Hydrocarbon composition (%)						
	C_1	C_2	C_3	*i*-C_4	C_4	C_5	C_6
Bush Hill	29.7	15.3	36.6	9.7	4.0	3.2	1.6
Bush Hill White	72.1	11.5	13.1	2.4	1.0	0.0	0.0
Bush Hill Yellow	73.5	11.5	11.6	2.0	1.0	0.1	0.0
Green Canyon White	66.5	8.9	15.8	7.2	1.4	0.1	0.1
Green Cayon Yellow	69.5	8.6	15.2	5.4	1.2	0.0	0.0
Haakon Mosby Mud Volcano	99.5	0.1	0.1	0.1	0.1	0.0	0.1

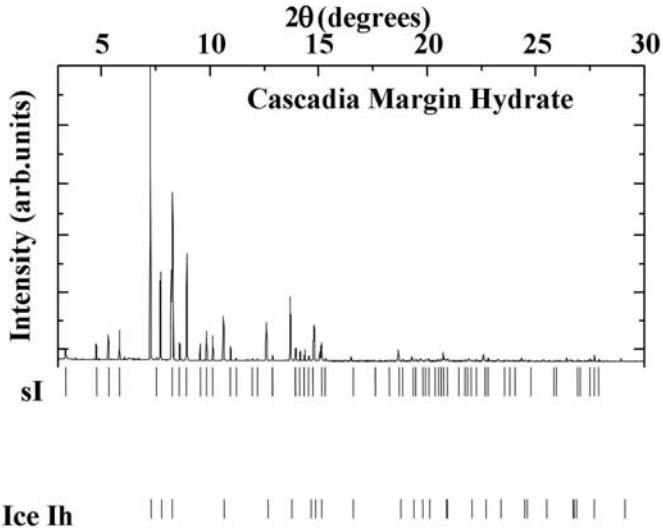

Figure 2: Powder diffraction pattern for the hydrate sample of Cascadia Margin, showing major constituents are ice Ih and hydrate sI.

ISSN 2995-8067 DOI: 10.61927/igmin265

Table 2: Powder diffraction data analysis of the Cascadia Margin Sample at P = 5.6 MPa, T = 85 K. In the 2θ range 1.6 to 30⁰, 78 discernible peaks are observed, of which 26 peaks are due to ice Ih and 52 peaks due to sI.

Ice Ih			Structure (I)		
(hkl)	d_{hkl}	I	(hkl)	d_{hkl}	I
(100)	3.9125	888	(110)	8.4382	42
(002)	3.6635	82	(200)	5.9569	22
(101)	3.4538	380	(210)	5.3304	89
(102)	2.6794	165	(211)	4.8611	91
(110)	2.2584	166	(310)	3.7651	10
(103)	2.0776	206	(222)	3.4406	205
(200)	1.9561	21	(320)	3.3001	68
(112)	1.9252	125	(321)	3.1786	357
(201)	1.8817	77	(400)	2.9734	46
(202)	1.7276	12	(410)	2.8871	98
(203)	1.5288	38	(330)	2.8061	67
(210)	1.4792	12	(421)	2.5966	43
(211)	1.4501	7	(332)	2.5369	9
(114)	1.4228	5	(430)	2.3795	6
(105)	1.3731	10	(510)	2.3349	4
(212)	1.3649	6	(520)	2.2092	19
(300)	1.3048	7	(530)	2.0408	53
(213)	1.2663	20	(531)	2.0106	31
(302)	1.2291	5	(442)	1.9841	14
(106)	1.1681	7	(532)	1.9305	58
(220)	1.1297	3	(620)	1.8908	29
(222)	1.0796	2	(540)	1.8588	8
(116)	1.0776	3	(444)	1.7171	1
(311)	1.0737	1	(552)	1.6193	2
(215)	1.0395	<1	(650)	1.5237	3
(313)	0.9924	7	(651)	1.5119	5
			(652)	1.4648	5
			(820)	1.4431	1
			(742)	1.4324	3
			(822)	1.4027	2
			(830)	1.3938	2
			(831)	1.3832	7
			(751)	1.3773	24
			(840)	1.3306	1
			(833)	1.3225	1
			(753)	1.3133	2
			(655)	1.2832	3
			(850)	1.2661	10
			(843)	1.2612	3
			(851)	1.2543	10
			(844)	1.2093	1
			(853)	1.2022	2
			(1000)	1.1963	2
			(950)	1.1554	1
			(953)	1.1096	1
			(864)	1.0964	1
			(865)	1.0648	4
			(963)	1.0601	1
			(1130)	1.0477	2
			(882)	1.0357	17
			(1132)	1.0278	4
			(1062)	1.0149	4
a = 4.5115 ± 0.0068 Å, c = 7.3566 ± 0.0001 Å, c/a = 1.6306 ± 0.0001 Å, V = 129. 672Å³			a = 11.91132 ± 0.0235 Å, V = 1689.955 Å³		

clathrate hydrates from the Pacific seafloor, collected during the research cruise SONNE 110, were found to predominantly contain sI structure, with the sample comprising 97.4% CH4, 2.6% H2S, and traces of CO_2, C_4H_6, and C_3H_8 [22].

Hydrates of Bush Hill, Gulf of Mexico

The Jolliet Field in Green Canyon 184 exemplifies a direct association between oil accumulation and thermogenic gas hydrate. Oil and gas are trapped in Pleistocene-Pliocene reservoir sands at depths of approximately 2-3 kilometers. The Bush Hill gas hydrate site, located on GC185 at the surface trace of a hydrocarbon-charged antithetic fault (27° 47.5' N, 91° 30.5' W), is near the Jolliet Field at a depth of about 540 meters. This natural mineral was collected off the southwestern coast of the United States. Analysis of this Gulf of Mexico mineral revealed it contains 72 to 74% methane, with the remainder being higher hydrocarbons (Table 1). A typical diffractogram (T = 150 K) is shown in Figure 3, and Table 3 lists the experimental d-spacings. The lattice parameters for ice Ih are: a = 4.5047 ± 0.00037 Å, c = 7.2412 ± 0.0001 Å, while the lattice parameter for sII is: a = 17.0888 ± 0.0004 Å. Although the Bush Hill samples primarily consist of sII and ice Ih, several peaks may originate from sI (a = 11.7346 ± 0.0300 Å) and sH (a = 11.4496 ± 0.3324 Å, c = 9.7064 ± 0.0330 Å), as detailed in Table 3.

Hydrates of Green Canyon, Gulf of Mexico

The Green Canyon, Gulf of Mexico minerals have been analyzed to contain 66 to 70% methane, with the remainder consisting of higher hydrocarbons, particularly ethylene and cyclohexane. A typical diffractogram (T = 150 K) is shown in Figure 4, and Table 4 lists the experimental d-spacings. The lattice parameters for ice Ih are: a = 4.5170 ± 0.00032 Å, c = 7.3665 ± 0.0001 Å, while the lattice parameter for structure II (sII) is: a = 17.2170 ± 0.0060 Å. Although the Green Canyon

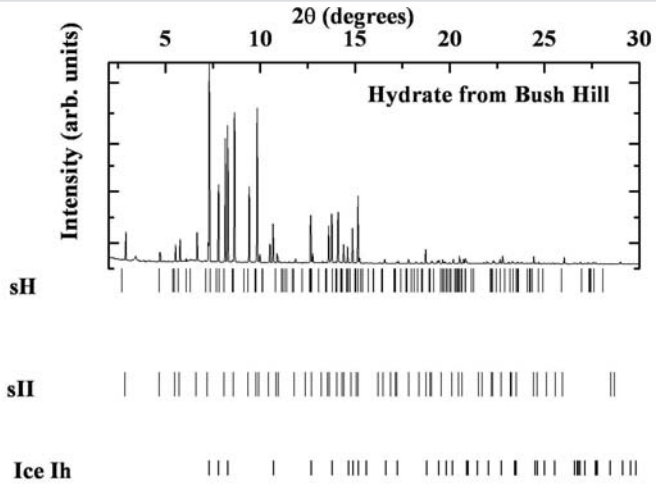

Figure 3: X-ray Powder diffraction pattern for the hydrate sample from Bush Hill, Gulf of Mexico. The major structures of the sample are ice Ih and hydrate sII.

ISSN 2995-8067 DOI: 10.61927/igmin265

Table 3: Powder diffraction data analysis of the Bush Hill Sample at P = 45 MPa, T = 93 K. In the 2θ range 1.6⁰ to 30⁰, 101 discernible peaks are observed, of which 27 peaks are due to ice Ih, 7 peaks due to sI, 45 peaks to sII, and remaining 22 peaks can be assigned to sH.

Ice Ih			Structure I			Structure II			Structure H		
(hkl)	d_{hkl}	I	(hkl)	d_{hkl}	I	(hkl)	d_{hkl}	I	(hkl)	d_{hkl}	I
(100)	3.8825	780	(110)	8.2947	36	(111)	9.7596	88	(201)	4.6787	7
(002)	3.6435	206	(421)	2.6057	16	(222)	6.0195	39	(102)	4.5076	9
(101)	3.4354	245	(1000)	1.1809	3	(311)	5.1375	44	(202)	3.6656	93
(102)	2.6622	104	(865)	1.0559	4	(222)	4.9308	26	(003)	3.4133	41
(110)	2.2477	213	(882)	1.0349	6	(400)	4.2615	105	(303)	2.4285	2
(103)	2.0657	131	(1132)	1.0257	1	(331)	3.9166	71	(544)	1.1841	2
(200)	1.9495	58	(1062)	0.9669	3	(422)	3.4860	424	(1000)	1.0521	1
(112)	1.9153	133				(333)	3.2881	640	(555)	1.0431	5
(201)	1.8804	213				(440)	3.0209	287	(627)	1.0203	1
(202)	1.7205	18				(531)	2.8904	628	(429)	0.9704	3
(203)	1.5232	60				(442)	2.8499	32			
(210)	1.4735	13				(620)	2.7051	60			
(211)	1.4545	14				(533)	2.6134	23			
(114)	1.4143	16				(622)	2.5797	6			
(105)	1.3718	21				(444)	2.4703	4			
(212)	1.3673	12				(711)	2.3972	14			
(300)	1.3005	10				(553)	2.2286	36			
(213)	1.2546	33				(800)	2.1394	3			
(302)	1.2254	9				(733)	2.0919	136			
(106)	1.1715	27				(644)	2.0696	99			
(220)	1.1259	5				(660)	2.0195	155			
(222)	1.0769	3				(822)	2.0158	91			
(311)	1.0657	8				(555)	1.9778	80			
(215)	1.0399	9				(842)	1.8693	18			
(313)	0.9896	10				(844)	1.7488	4			
						(666)	1.6490	10			
						(953)	1.5992	19			
						(1042)	1.5648	11			
						(11111)	1.5405	4			
						(1131)	1.4976	11			
						(1044)	1.4929	5			
						(1060)	1.4690	12			
						(973)	1.4449	8			
						(1200)	1.4284	4			
						(1064)	1.3827	2			
						(1082)	1.3228	1			
						(1155)	1.3113	5			
						(1173)	1.2817	13			
						(1084)	1.2786	4			
						(888)	1.2374	6			
						(1264)	1.2281	7			
						(1420)	1.2039	4			
						(1371)	1.1588	6			
						(1444)	1.1386	2			
						(999)	1.1003	22			
a = 4.5047 ± 0.0037 Å, c = 7.2412 ± 0.0001 Å, c/a = 1.6075 ± 0.0001 Å, V = 127.256 Å³			a = 11.7346 ± 0.0300 Å, V = 1615.844 Å³			a = 17.0888 ± 0.0040 Å, V = 4990.401 Å³			a = 11.4496 ± 0.3324 Å, c = 9.7064 ± 0.0330 Å, c/a = 0.8478 ± 0029, V = 1101.978 Å³		

ISSN 2995-8067 DOI: 10.61927/igmin265

samples primarily consist of sII and ice Ih, several peaks suggest the presence of structure I (sI) with lattice parameters a = 11.9292 ± 0.0380 Å and structure H (sH) with lattice parameters a = 11.7284 ± 0.0451 Å and c = 9.6717 ± 0.0001 Å, as detailed in Table 4.

Spurred by this work, several theoretical and experimental efforts have ensued. Notable ones are summarized as follows: Using grand canonical Monte Carlo simulations, Papadimitriou *et al* have shown that above 380 MPa, 3.0 wt% hydrogen storage could be achieved [23]. The study of Bourry *et al* on natural hydrates from the African margin indicates a preponderance of biogenic methane with a minor composition of CO_2 and H_2S and at elevated temperatures, the thermal expansion approached that of ice [24]. Raman spectroscopic investigation on hydrates extracted from the West African

Table 4: Powder diffraction data analysis of the hydrate sample from the Northern Gulf of Mexico at P = 0.15 MPa, T = 90 K. In the 2θ range 1.6^0 to 30^0, 102 peaks are observed of which 26 peaks are due to ice Ih, 45 peaks due to sII, and remaining 26 and 5 peaks can correspondingly be assigned to sH and sI.

Ice Ih			Structure I			Structure II			Structure H		
(hkl)	d_{hkl}	I	(hkl)	d_{hkl}	I	(hkl)	d_{hkl}	I	(hkl)	d_{hkl}	I
(100)	3.9134	293	(110)	8.4382	25	(111)	9.9722	9	(100)	10.1690	1
(002)	3.6767	161	(211)	4.8799	5	(220)	6.0947	7	(001)	9.6712	1
(101)	3.4555	396	(320)	3.3076	226	(311)	5.1963	24	(110)	5.8622	1
(102)	2.6803	58	(410)	2.9062	94	(222)	4.9744	22	(200)	5.0478	2
(110)	2.2592	309	(430)	2.3857	1	(400)	4.3066	47	(111)	5.0085	1
(103)	2.0777	128				(331)	3.9522	38	(002)	4.8799	5
(200)	1.9563	13				(422)	3.5179	92	(201)	4.4865	1
(112)	1.9252	61				(511)	3.3159	161	(102)	4.3804	1
(201)	1.8791	6				(440)	3.0435	184	(112)	3.6704	25
(202)	1.7285	7				(531)	2.9136	167	(300)	3.3778	20
(203)	1.5290	15				(442)	2.8699	12	(214)	2.0000	2
(210)	1.4788	23				(620)	2.7207	94	(510)	1.8229	1
(211)	1.4501	4				(533)	2.6259	15	(225)	1.6391	1
(114)	1.4203	7				(622)	2.5965	2	(008)	1.2087	1
(105)	1.3770	11				(551)	2.4104	6	(803)	1.1854	1
(212)	1.3722	4				(553)	2.2427	15	(550)	1.1764	4
(300)	1.3037	10				(800)	2.1519	2	(544)	1.1510	1
(213)	1.2663	43				(733)	2.1044	65	(635)	1.1045	3
(302)	1.2294	4				(660)	2.0296	108	(824)	0.9924	5
(106)	1.1764	4				(555)	1.9882	32	(627)	0.9699	1
(220)	1.1301	7				(842)	1.8791	32			
(222)	1.0789	5				(664)	1.8302	12			
(116)	1.0735	2				(951)	1.6652	5			
(311)	1.0697	2				(666)	1.6567	3			
(215)	1.0433	4				(953)	1.6060	7			
(313)	0.9924	4				(1042)	1.5724	2			
						(880)	1.5311	5			
						(955)	1.5050	2			
						(1060)	1.4766	4			
						(1133)	1.4607	4			
						(1200)	1.4350	1			
						(1064)	1.3973	12			
						(975)	1.3832	4			
						(991)	1.3485	2			
						(1082)	1.3282	3			
						(1155)	1.3170	2			
						(1173)	1.2873	3			
						(1084)	1.2837	1			
						(1333)	1.2598	10			
						(888)	1.2431	3			
						(1351)	1.2333	2			
						(1371)	1.1606	1			
						(1444)	1.1413	1			
Ice Ih: 26 peaks a = 4.5170 ± 0.0032 Å, c = 7.3665 ± 0.0001 Å, c/a = 1.6308 ± 0.0001 Å, V = 130.162Å^3			sI: 5 peaks a = 11.9292 ± 0.0380 Å, V = 1697.604 Å^3			sII: 45 peaks a = 17.2170 ± 0.0060 Å, V = 5103.538 Å^3			sH: 26 peaks a = 11.7284 ± 0.0451 Å, c = 9.6717 ± 0.0001 Å, c/a = 0.8246 ± 0001 V = 1152.148 Å^3		

ISSN 2995-8067 DOI: 10.61927/igmin265

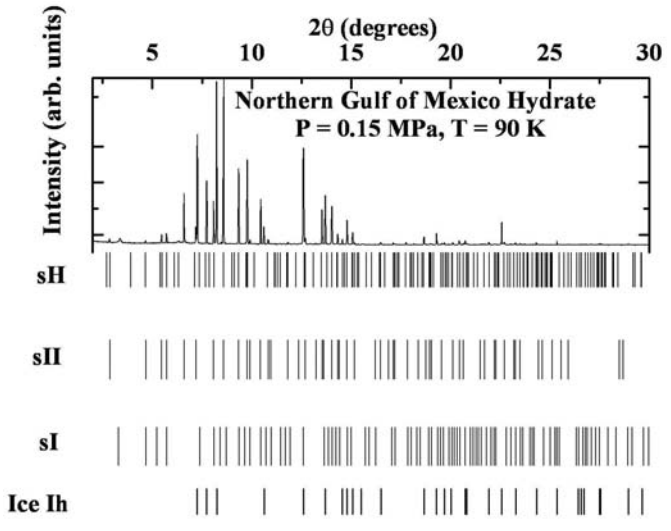

Figure 4: Powder diffraction pattern for the hydrate sample from Green Canyon, Northern Gulf of Mexico. The major structures of the sample are ice Ih and hydrate sII. A major conclusion gleaned from the powder pattern is that the quantity of hydrate samples is much more than ice.

margin in the South Atlantic Ocean (ZaiAngo and Neris II) and from Hakon Mosby Mud Volcano (Norwegian Sea) exhibit a major concentration of CH_4 [25].

Present studies carried out on the hydrate samples recovered from Bush Hill and Green Canyon show the existence of a minor sH structure. Future studies such as high energy high-resolution nuclear techniques are needed to clearly identify the natural gases present in natural hydrates.

Conclusion

In the present study, structural analyses of natural gas hydrate minerals were conducted using high-resolution angular dispersive X-ray diffraction at the BESSRC CAT ID 11-D beam-line of the Advanced Photon Source. It was determined that the gas hydrate samples from the Cascadia Margin consist of structure I (sI) and ice Ih, while those from Bush Hill and Green Canyon contain structure II (sII) and ice Ih, along with traces of structure H (sH). Ice Ih is found to coexist in all the natural mineral samples. The variation in the concentration of sI, sII, and sH in these samples indicates significant differences in the types and concentrations of natural gases present at these geographically distinct locations. The stronger ice peaks in the Cascadia Margin samples suggest a lower concentration of hydrates compared to the Bush Hill and Green Canyon samples, which contain more than 60% hydrates.

Acknowledgement

We are grateful to Drs. Ken Grabowski, David Knies, and B.B. Rath for encouragement and helpful discussions. Also, we acknowledge the assistance of Dr. Jennifer A. Linton, BESSRC CAT, Materials Science Division, Argonne National Laboratory in setting up the experiments.

References

1. Coffin RB, Lamontagne R, Rose-Pehrsson S, Grabowski KS, Knies DL, Qadri SB, Yesinowski JP, Pohlman JW, Yousuf M, Linton JA. Ocean Floor Methane Gas Hydrate Exploration. NRL Review. 2002;112.
2. Yousuf M, Qadri SB, Knies DL, Grabowski KS, Coffin RB, Pohlman JW. Novel results on structural investigations of natural minerals of clathrate hydrates. Appl Phys A. 2003;78:925-939.
3. Haq BU. Methane in the Deep Blue Sea. Science. 1999;285:543-544.
4. Brooks JM, Kennicutt II MC, Fay RR, McDonald TJ, Sassen R. Thermogenic Gas Hydrates in the Gulf of Mexico. Science. 1984;225:409-411.
5. Kennicutt II MC, Brooks JM, Denoux GJ. Leakage of deep, reservoired petroleum to the near surface on the Gulf of Mexico continental slope. Marine Chem. 1988;24:39-59.
6. MacDonald IR, Guinasso NL Jr, Sassen R, Brooks JM, Lee L, Scott KT. Gas hydrate that breaches the sea floor on the continental slope of the Gulf of Mexico. Geology. 1994;22:699-702.
7. McMullan RK, Jeffery GA. Polyhedral Clathrate Hydrates. IX. Structure of Ethylene Oxide Hydrate. J Chem Phys. 1965;42:2725-2732.
8. Mak TCW, McMullan RK. Polyhedral Clathrate Hydrates. X. Structure of the Double Hydrate of Tetrahydrofuran and Hydrogen Sulfide. J Chem Phys. 1965;42:2732-2737.
9. Udachin KA, Ripmeester JA. A complex clathrate hydrate structure showing bimodal guest hydration. Nature. 1999;397:420-423.
10. Ripmeester JA, Ratcliffe CI. The diverse nature of dodecahedral cages in clathrate hydrates as revealed by 129Xe and 13C NMR spectroscopy: CO2 as a small-cage guest. Energy Fuels. 1998;12:197-200.
11. Sloan ED. Gas Hydrates: Review of Physical/Chemical Properties. Energy Fuels. 1998;12:191.
12. Holbrook WS, Hoskins H, Wood WT, Stephen RA, Lizarralde D. Methane Hydrate and Free Gas on the Blake Ridge from Vertical Seismic Profiling. Science. 1996;273:1840-1843.
13. Shoji H, Langway CC. Air hydrate inclusions in fresh ice core. Nature. 1982;298:548-550.
14. Makogon YF, Makogon TY, Holditch SA. Gas Hydrate: Challenges for the Future. In: Holder GD, Bishnoi PR, editors. Annals of the New York Academy of Sciences. 2000;912:777.
15. Rogner HH. An Assessment of World Hydrocarbon Resources. Annu Rev Energy Environ. 1997;22:217-262.
16. Sassen R, MacDonald IR, Requejo AG, Guinasso NL Jr, Kennicutt II MC, Sweet ST, Brooks JM. Organic geochemistry of sediments from chemosynthetic communities, Gulf of Mexico slope. Geo-Marine Lett. 1994;14:110-119.
17. Pauling L. The Nature of the Chemical Bond and The Structure of Molecules and Crystals. Ithaca, NY: Cornell University Press; 1960.
18. Jeffrey GA. Inclusion Compounds. Vol. 1: Structural Aspects of Inclusion Compounds Formed by Inorganic and Organometallic Host Lattices. Atwood JL, Davies JED, MacNichol DD, editors. Academic Press; 1984;135.
19. Sloan ED Jr. Clathrate Hydrates of Natural Gases. New York: Marcel Dekker, Inc.; 1998.
20. Rahman A, Stillinger FH. Hydrogen-bond patterns in liquid water. J Am Chem Soc. 1973;95:7943.
21. Khan A. Theoretical studies of tetrakaidecahedral structures of (H2O)24, (H2O)25 and (H2O)26 clusters. Chem Phys Lett. 1996;253:299-304.
22. Beno MA, Kurtz C, Munkholm A, Rüt U, Engbretson M, Jennings G, Linton

J, Knapp GS, Montano PA. Elliptical multipole wiggler beamlines at the advanced photon source. Nucl Instrum Methods Phys Res A. 2001;467-468:694.

23. Gutt C. Europhys Lett. 1999;48:269.

24. Papadimitriou NI, Tsimpanogiannis IN, Papaioannou A Th, Stubos AK. Evaluation of the Hydrogen-Storage Capacity of Pure H2 and Binary H2-THF Hydrates with Monte Carlo Simulations. J Phys Chem C. 2008;112:10294.

25. Bourry C, Chazallon B, Charlou JL, Donval JP, Ruffine L, Henry P, Geli L, Çagatay MN, İnan S, Moreau M. Free gas and gas hydrates from the Sea of Marmara, Turkey: Chemical and structural characterization. Geophys Res Lett. 2009;264:197-206.

How to cite this article: Yousuf M, Qadri SB. High Resolution X-ray Diffraction Studies of the Natural Minerals of Gas Hydrates and Occurrence of Mixed Phases. IgMin Res. November 04, 2024; 2(11): 889-896. IgMin ID: igmin265; DOI: 10.61927/igmin265; Available at: igmin.link/p265

Publisher note: Thank you for providing this insightful research study—it's a valuable asset that will empower us in our future undertakings.

INSTRUCTIONS FOR AUTHORS

IgMin Research - A BioMed & Engineering Open Access Journal is a prestigious multidisciplinary journal committed to the advancement of research and knowledge in the expansive domains of Biology, Medicine, and Engineering. With a strong emphasis on scholarly excellence, our journal serves as a platform for scientists, researchers, and scholars to disseminate their groundbreaking findings and contribute to the ever-evolving landscape of Biology, Medicine and Engineering disciplines.

For book and educational material reviews, send them to IgMin Research, at support@igminresearch.us. The Copyright Clearance Centre's Rights link program manages article permission requests via the journal's website (https://www.igminresearch.com). Inquiries about Rights link can be directed to info@igminresearch.us or by calling +1 (860) 967-3839.

https://www.igminresearch.com/pages/publish-now/author-guidelines

APC

In addressing Article Processing Charges (APCs), IgMin Research: recognizes their significance in facilitating open access and global collaboration. The APC structure is designed for affordability and transparency, reflecting the commitment to breaking financial barriers and making scientific research accessible to all.

At IgMin Research - A BioMed & Engineering Open Access Journal, fosters cross-disciplinary communication and collaboration, aiming to address global challenges. Authors gain increased exposure and readership, connecting with researchers from various disciplines. The commitment to open access ensures global availability of published research. Join IgMin Research - A BioMed & Engineering Open Access Journal at the forefront of scientific progress.

https://www.igminresearch.com/pages/publish-now/apc

WHY WITH US

IgMin Research | A BioMed & Engineering Open Access Journal employs a rigorous peer-review process, ensuring the publication of high-quality research spanning STEM disciplines. The journal offers a global platform for researchers to share groundbreaking findings, promoting scientific advancement.

JOURNAL INFORMATION

Journal Full Title: IgMin Research-A BioMed & Engineering Open Access Journal
Journal NLM Abbreviation: IgMin Res
Journal Website Link: https://www.igminresearch.com
Topics Summation: 150
Subject Areas: Biology, Engineering, Medicine and General Science
Organized by: IgMin Publications Inc.

Regularity: Monthly
Review Type: Double Blind
Publication Time: 14 Days
GoogleScholar: https://www.igminresearch.com/gs
Plagiarism software: iThenticate
Language: English
Collecting capability: Worldwide

License: Open Access by **IgMin Research** is licensed under a Creative Commons Attribution 4.0 International License. Based on a work at **IgMin Publications Inc**.

Online Manuscript Submission:
https://www.igminresearch.com/submission or can be mailed to submission@igminresearch.us